Highly active and stable alumina supported nickel nanoparticle catalysts for dry reforming of methane

Zeyu Shang[a], Shiguang Li[b], Ling Li[c], Guozhu Liu[c], Xinhua Liang[a,*]

[a] Department of Chemical and Biochemical Engineering, Missouri University of Science and Technology, Rolla, MO 65409, United States
[b] Gas Technology Institute, 1700 S Mount Prospect Road, Des Plaines, IL 60018, United States
[c] Key Laboratory for Green Chemical Technology of Ministry of Education, School of Chemical Engineering and Technology, Tianjin University, Tianjin 300072, PR China

ARTICLE INFO

ABSTRACT

A highly stable and extremely active nickel (Ni) nanoparticle catalyst, supported on porous γ-Al$_2$O$_3$ particles, was prepared by atomic layer deposition (ALD). The catalyst was employed to catalyze the reaction of dry reforming of methane (DRM). The catalyst initially gave a low conversion at 850 °C, but the conversion increased with an increase in reaction time, and stabilized at 93% (1730 L h^{-1} g$_{Ni}$$^{-1}$ at 850 °C). After regeneration, the catalyst showed a very high methane reforming rate (1840 L h^{-1} g$_{Ni}$$^{-1}$ at 850 °C). The activated catalyst showed exceptionally high catalytic activity and excellent stability of DRM reaction in over 300 h at temperatures that ranged from 700 °C to 850 °C. The excellent stability of the catalyst resulted from the formation of NiAl$_2$O$_4$ spinel. The high catalytic activity was due to the high dispersion of Ni nanoparticles deposited by ALD and the reduction of NiAl$_2$O$_4$ spinel to Ni during the DRM reaction at 850 °C. It was verified that NiAl$_2$O$_4$ can be reduced to Ni in a reductive gas mixture (i.e., carbon monoxide and hydrogen) during the reaction at 850 °C, but not by H$_2$ alone.

1. Introduction

Methane reforming with carbon dioxide (CH$_4$ + CO$_2$ → 2H$_2$ + 2CO), also called dry reforming of methane (DRM), obtained considerable attention due to the advances in shale gas recovery [1,2]. DRM is important because the two main greenhouse gases (carbon dioxide and methane) could be converted to syngas (carbon monoxide and hydrogen) in this reaction process. The H$_2$/CO ratio is always lower than 1 due to a reverse water-gas shift reaction (CO$_2$ + H$_2$ ⇌ CO + H$_2$O). This gas mixture could be used to blend streams from methane steam reformation to produce syngas with the desired H$_2$/CO ratio, which could be applied in the Fischer–Tropsch (FT) synthesis [3,4]. Different metal catalysts (e.g., Rh [5,6], Pt [7,8], Ir [9], Pd [10], Ru [11,12], and Ni [13,14]) were employed to catalyze the DRM reaction. Among them, noble metal catalysts showed better resistance to coking, as compared to Ni catalysts [15,16]. However, due to the limited availability and high cost of noble metals, it was considered desirable to develop a Ni-based catalyst.

The main disadvantage of the Ni catalyst for DRM reaction is deactivation, due to coking and sintering of Ni metal nanoparticles to form larger particles with lower catalytic activity [17]. Coking could be decreased by running the reaction at high temperatures and using small Ni particles, because their step edges are small enough to limit carbon nucleation and growth [4,18]. However, the aggregation of small Ni nanoparticles will be more extreme at higher reaction temperatures. Therefore, there is a trade-off when Ni nanoparticles are used at higher temperatures. The supported Ni catalysts are normally synthesized by an impregnation method using an aqueous solution of nickel nitrate hexahydrate (Ni(NO$_3$)$_2$·6H$_2$O) [13,14,19–21]. The Ni nanoparticles that are synthesized by the impregnation method are relatively large, typically tens of nanometers [22–24]. They have lower Ni surface areas, compared to smaller Ni nanoparticles, and are easier to get coked.

Atomic layer deposition (ALD) is a self-limiting and self-terminating gas phase deposition technique that has been successfully demonstrated for the synthesis of metal nanoparticles (e.g., Pd and Pt) on different substrates [25,26]. Small Ni nanoparticles (∼3 nm) could be synthesized by ALD and have been demonstrated to be an excellent catalyst with high catalytic activity for catalyzing hydrogenation of propylene [27]. In addition, the ALD Ni nanoparticles strongly interacted with the substrate, which was more stable, when compared to the Ni nanoparticles prepared

by conventional methods. Alumina was demonstrated to be a better catalyst support for the Ni catalyst, as compared to some other catalyst supports (e.g., SiO_2 and $MgO-SiO_2$). This could be due to the fact that the alumina support increased the overall basicity of the supported Ni catalyst and there was a stronger metal-support interaction between the Ni and alumina support [28,29].

Gould et al. [30] deposited Ni nanoparticles (~3 nm) on dense alumina nanoparticles by ALD to catalyze the DRM reaction and applied porous alumina film obtained from aluminum alkoxide (alucone) molecular layer deposition (MLD) films to stabilize the Ni nanoparticles. The idea was to use ALD to prepare highly dispersed Ni nanoparticles with high catalytic activity and to use porous alumina films to encapsulate the Ni nanoparticles for greater thermal stability. Their results showed that five cycles of alucone MLD could increase the thermal stability and steady-state activity of the catalyst. However, previous studies by Liang et al. indicated that the porous alumina film formed from ten cycles of alucone MLD by calcination could not completely encapsulate 1.8 nm average size Pt particles [31]. Similarly, it would be difficult to use porous alumina films obtained from 5 cycles of alucone MLD coating to encapsulate 3 nm Ni nanoparticles. Therefore, the increase in catalyst stability, with five cycles of MLD coating, should not result from stabilization of Ni particles by alumina film encapsulation. The interaction between the Ni nanoparticles and the deposited alumina film could be the key. In the study by Gould et al., dense alumina nanoparticles were used as catalyst support [30]. We hypothesize that the catalytic performance could be very different if we used porous alumina particles as the catalyst support. There will be more interaction between the Ni nanoparticles and the porous alumina support (as schematically shown in Fig. S1), since there is more interfacial contact between nanoparticles and the concave surface (porous support), compared to the case of a convex surface (dense particle support). Thus, the thermal stability of the highly dispersed ALD Ni nanoparticles would be improved. In this study, we synthesized a porous $\gamma-Al_2O_3$ supported Ni nanoparticles catalyst using the ALD technique. The DRM reaction was initially carried out at 850 °C, to activate the catalyst, and then run at different temperatures. The reduction mechanism of $NiAl_2O_4$ spinel was studied.

2. Experimental

2.1. Materials

Dense alumina nanoparticles (50–100 nm, gamma phase) and porous $\gamma-Al_2O_3$ particles were purchased from Sigma-Aldrich and Alfa Aesar, respectively. The porous alumina particles were 40 μm in diameter, with a Brunauer–Emmett–Teller (BET) surface area of 95.5 m^2/g. The dense alumina nanoparticles had a BET surface area of 137 m^2/g. Bis(cyclopentadienyl)nickel ($NiCp_2$) and $Ni(NO_3)_2 \cdot 6H_2O$ were purchased from Alfa Aesar and Fisher Scientific, respectively.

2.2. Catalyst preparation and characterization

Ni nanoparticle ALD was carried out using $NiCp_2$ and hydrogen as precursors at 300 °C in a fluidized bed reactor. The ALD reactor system has been previously described in detail [32]. Both porous $\gamma-Al_2O_3$ particles and dense alumina nanoparticles were used as the substrates and one cycle of Ni ALD was applied. These two catalysts were labeled as ALD Ni/$\gamma-Al_2O_3$, and ALD Ni/NP-Al_2O_3, respectively. To obtain a better characterization result, a porous $\gamma-Al_2O_3$ supported Ni catalyst with four cycles of Ni ALD (a Ni loading of 4 wt.%) was synthesized and labeled as ALD 4-Ni/$\gamma-Al_2O_3$. For comparison, Ni nanoparticles supported on porous $\gamma-Al_2O_3$ par-

ticles were also prepared by the incipient wetness (IW) method. An aqueous solution of $Ni(NO_3)_2$ $6H_2O$ was added to the porous $\gamma-Al_2O_3$ particles and dried at 110 °C, while stirring continuously. The sample was then calcined in air at 550 °C for 6 h. The catalyst prepared by the IW method was labeled as IW Ni/$\gamma-Al_2O_3$.

The Ni loadings of different catalysts were measured by inductively coupled plasma-atomic emission spectroscopy (ICP–AES, Model ARL 34101, Thermo Electron, Waltham, MA).

The average size and dispersion of the Ni nanoparticles supported on alumina nanoparticles were observed by transmission electron microscopy (TEM) with a FEI Tecnai F20 TEM.

In order to measure the coke content of the used catalyst, derivative thermogravimetric (DTG) analyses of the samples were made using a TA Instruments Q50 thermogravimetric analyzer. The DTG analyses were carried out with an air (40 mL/min) and N_2 (40 mL/min) stream. The temperature was increased from room temperature to 200 °C, at a heating rate of 10 °C/min, and kept at 200 °C for 60 min, and then increased to 1000 °C at the same rate.

X-Ray diffraction (XRD) spectra were recorded on a Philips X-Pert Multi-purpose Diffractometer, using Cu Kα 1 radiation (λ=0.15416 nm).

X-ray photoelectron spectroscopy (XPS) measurements were performed using a Kratos Axis 165 X-ray photoelectron spectrometer with a monochromatic Al Kα radiation (h = 1486.6 eV). All binding energy values were corrected based on a C (1s) peak at 284.5 eV.

H_2-temperature programmed reduction (TPR) tests were performed using an AMI-300. Typically, 100 mg of the sample were charged in a quartz tube and reduced up to 900 °C at a heating rate of 10 °C/min in a stream of 10% H_2 in Ar. The ALD Ni/$\gamma-Al_2O_3$ and ALD Ni/NP-Al_2O_3 samples were oxidized at 550 °C for 1 h before the TPR test.

2.3. General procedure for dry reforming of methane

Different amounts of various catalysts were loaded into a quartz tube reactor (10 mm diameter) to keep the Ni content consistent (~0.64 mg). Quartz wool was employed to support the catalysts. The catalysts, using porous $\gamma-Al_2O_3$ as supports, were diluted with 0.5 g of quartz sands (60–120 mesh) and were well distributed in the quartz sands. A thermal couple was applied to measure the temperature. The ALD synthesized catalysts were oxidized at 550 °C to remove any residual organic components from the Ni ALD precursor. All of the catalysts were reduced with 20% H_2 and 80% Ar (with a total flow rate of 100 sccm) at 700 °C for 1 h before the DRM reaction. CH_4 and CO_2 that were balanced with Ar (20% CH_4, 20% CO_2, and 60% Ar, with a total flow rate of 100 sccm), were introduced into the reactor at different temperatures for a DRM reaction. The catalysts were regenerated after the reaction and applied to catalyze the DRM reaction again. In a typical regeneration process, the catalyst was first oxidized in 20% O_2 and 80% Ar at 700 °C for 1 h and then reduced in 20% H_2 and 80% Ar at the same temperature for 1 h. The gas flow rates were controlled by MKS® mass flow controllers. The reaction products were analyzed by an online gas chromatograph (SRI 8610C) equipped with a 6-foot HAYESEP D column, a 6-foot MOLECULAR SIEVE 13X column, and a thermal conductivity detector (TCD).
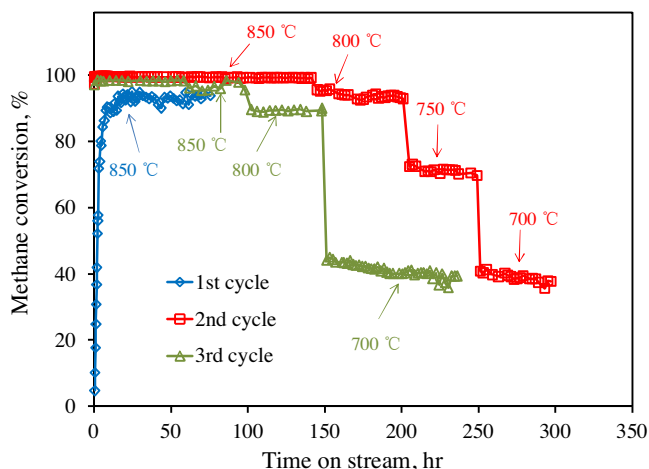
3. Results and discussion

3.1. Catalytic performance

The ALD Ni/$\gamma-Al_2O_3$ catalyst was first employed to catalyze the DRM. Fig. 1 shows the DRM reaction results at different temperatures as catalyzed by ALD Ni/$\gamma-Al_2O_3$. In the first cycle (here, one

Table 1

Catalytic activities comparison of different Ni/Al$_2$O$_3$ catalysts in DRM reaction.

| Catalyst	Methane reforming rate (L h^{-1} g$_{Ni}$$^{-1}$)				References
	850 °C	800 °C	750 °C	700 °C	
ALD Ni/γ-Al$_2$O$_3$	1840	1740	1320	720[a]	This work
Ni/γ-Al$_2$O$_3$	N/A	157	N/A	137	[36]
Inverse Ni/Al$_2$O$_3$ catalyst	N/A	1500	N/A	N/A	[35]
ALD Ni/dense γ-Al$_2$O$_3$	N/A	N/A	N/A	700	[30]

[a] The results were tested after about 250 h of reaction at high temperatures.

Fig. 1. Methane conversion of dry reforming of methane catalyzed by ALD Ni/γ-Al$_2$O$_3$ at different temperatures.

Fig. 2. Methane conversion of dry reforming of methane catalyzed by IW Ni/γ-Al$_2$O$_3$ at different temperatures.

cycle means testing at different temperatures without regeneration), the reaction was carried out at 700 °C, but no conversion was observed. The temperature of the DRM reaction was then increased to 850 °C, while the methane conversion kept increasing during the first 10 h, and then stabilized at ~93%. This increase could have been due to the activation of the catalyst. After running at 850 °C for 75 h, the catalyst was regenerated at 700 °C. In the second cycle, the methane conversion was 99% at 850 °C, and did not decrease in 140 h. This excellent stability could have been due to the fact that the sintering of Ni nanoparticles would be inhibited by the porous structure of the catalyst support and the strong interaction between the Ni nanoparticles and the catalyst support. When the reaction temperature was decreased to 800 °C, the methane conversion decreased to 95%, but only slightly decreased to 93% after 50 h of reaction. The methane conversion decreased to 72%, after the reaction temperature had decreased to 750 °C, and slightly decreased with an increase in the reaction time (70% after about 50 h). The reaction temperature then decreased further to 700 °C, while the methane conversion decreased to 40%, and then decreased slightly to 38% after about 50 h of reaction. Table 1 shows the methane reforming rates in the DRM reaction, for the second cycle of DRM reaction, which were calculated from the methane conversion (shown in Fig. 1), gas flow rate, and catalyst loading. The methane reforming rate at 850 °C in the second cycle was as high as 1840 L h^{-1} g$_{Ni}$$^{-1}$. This value could have been underestimated, since the methane conversion was pretty close to 100%. The third cycle showed results similar to those of the second cycle. This series of experiments, showed that the decreases in methane conversion at each temperature level should not have been due to the sintering. Otherwise, the performance of the catalyst in the third cycle would have been worse than that in the second cycle. It is believed that this decrease resulted from a slight coking on the catalyst. The catalyst color changed to black after the reaction due to coking (Fig. S2).
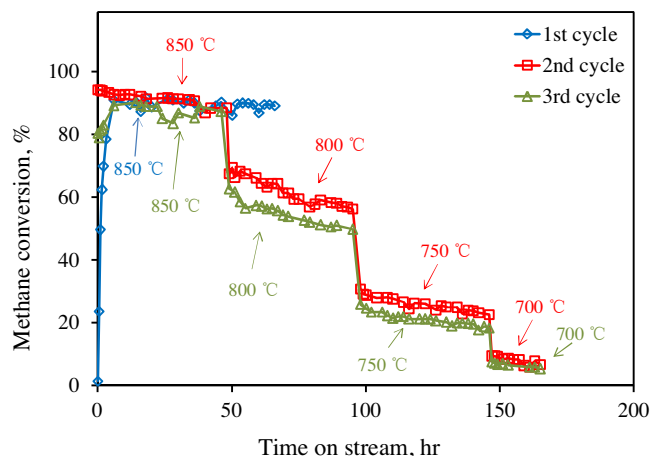
In previously reported studies of DRM, a reaction was normally carried out in a temperature range of 700 °C to 800 °C [19,20,30,33–35]. Only a few reports studied DRM reactions at 850 °C, since Ni nanoparticles would aggregate to form larger particles at those high temperatures. In this study, it was found that it was beneficial to run the DRM reaction at 850 °C, since the ALD Ni/γ-Al$_2$O$_3$ catalyst can be activated at that high temperature. In Table 1, the activity of the ALD Ni/γ-Al$_2$O$_3$ catalyst was compared with some other Ni/Al$_2$O$_3$ catalysts synthesized by other groups. Wang et al. [36] synthesized a gamma-alumina supported Ni catalyst by a wetness impregnation method and showed methane reforming rates of 137 L h^{-1} g$_{Ni}$$^{-1}$ and 157 L h^{-1} g$_{Ni}$$^{-1}$ at 700 °C and 800 °C, respectively. The porous alumina coated Ni nanoparticles, supported on dense alumina nanoparticles synthesized by Gould et al., gave a methane reforming rate of 700 L h^{-1} g$_{Ni}$$^{-1}$ at 700 °C [30]. Baktash et al. [35] synthesized an inverse catalyst with Ni nanoparticles encapsulated with alumina that gave a maximum methane reforming rate of 1500 L h^{-1} g$_{Ni}$$-1$ at 800 °C. In our study, the ALD Ni/γ-Al$_2$O$_3$ catalyst showed methane reforming rates of 1840 L h^{-1} g$_{Ni}$$^{-1}$ at 850 °C, 1740 L h^{-1} g$_{Ni}$$^{-1}$ at 800 °C, and 720 L h^{-1} g$_{Ni}$$^{-1}$ at 700 °C even after several hundreds of hours of reaction at high temperatures, which was still higher than the value reported by Gould et al. [30]. Clearly, the porous alumina supported ALD Ni nanoparticles showed much better activity, as compared to other catalysts reported previously.

To verify that ALD is a better way to prepare supported Ni nanoparticles catalysts, as compared to the traditional impregnation method, an IW Ni/γ-Al$_2$O$_3$ catalyst was employed to catalyze the DRM reactions (results shown in Fig. 2). The corresponding methane reforming rates of the second cycle of the DRM reaction are shown in Table 2. The reaction was first carried out at 850 °C. The catalyst was activated at the beginning of the reaction, and then, the methane conversion was kept at about 90%. Between each cycle, the catalyst was regenerated by following the same procedures that are mentioned above. In the second cycle, the methane

Table 2
Rate of dry reforming of methane and H_2/CO ratio catalyzed by three different catalysts at different temperatures.

Catalyst	CH_4 reforming rate ($L\,h^{-1}\,g_{Ni}^{-1}$)				H_2/CO ratio in the product			
	850 °C	800 °C	750 °C	700 °C	850 °C	800 °C	750 °C	700 °C
ALD Ni/γ-Al₂O₃	1840	1740	1320	720	0.82	0.78	0.68	0.55
IW Ni/γ-Al₂O₃	1700	1150	480	150	0.70	0.61	0.51	0.38
ALD Ni/NP-Al₂O₃	1380	850	410	190 (706)[a]	0.74	0.73	0.71	0.65

Note: The results in this table were calculated based on the second cycle of DRM reaction for all three catalysts.

[a] The value in brackets was calculated based on the result of DRM reaction carried out at 700 °C directly after reduction without running at higher temperatures.
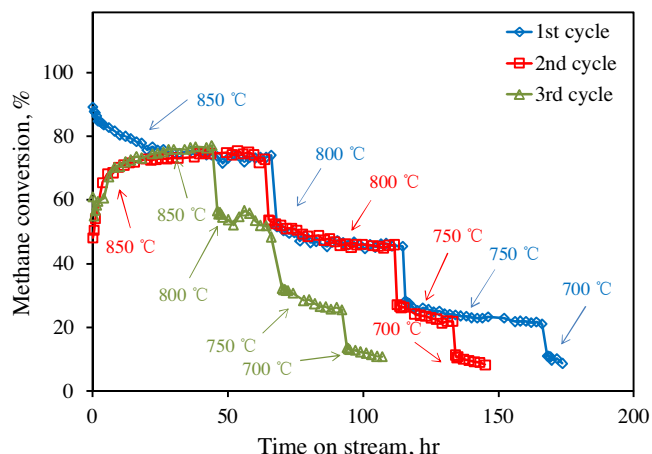
Fig. 3. Methane conversion of dry reforming of methane catalyzed by ALD Ni/NP-Al₂O₃ at different temperatures.

conversion was decreased from 94% to 88% in 48 h at 850 °C. The methane conversion decreased to 69% after the reaction temperature decreased to 800 °C, and decreased further to 56% in 48 h. The conversions of methane were lower than 30% and 10% at 750 °C and 700 °C, respectively. This catalyst showed lower stability and much lower activity, as compared to the ALD Ni/γ-Al₂O₃. In the third cycle, the performance of the catalyst was much worse. The lower catalytic activity and stability of the IW Ni/γ-Al₂O₃ catalyst could have been caused by two things: (1) the Ni nanoparticles synthesized by the IW method were much larger than the ALD-deposited Ni nanoparticles, which would have had lower catalytic activity due to a lower reactive surface area, and coking formation was easier; and (2) the bonding force between the Ni nanoparticles and the catalyst support for the IW Ni/γ-Al₂O₃ catalyst could have been weaker than that of the ALD Ni/γ-Al₂O₃ catalyst, since the Ni nanoparticles strongly interacted with the substrate in the ALD process.

To check the effect of porous catalyst support on the DRM reaction, the ALD Ni/NP-Al₂O₃ sample was also used to catalyze the DRM reaction. As shown in Fig. 3, the dense substrate supported catalyst showed high catalytic activity at the beginning, but no gradual increase of conversion when the reaction was carried out at 850 °C. This means that the catalysts can be activated very easily. Thus, it is reasonable to hypothesize that there was a much stronger interaction between the Ni nanoparticles and the porous γ-Al₂O₃ support for ALD Ni/γ-Al₂O₃ catalyst, as compared to the ALD Ni/NP-Al₂O₃ catalyst. After 60 h of reaction at 850 °C, the methane conversion decreased from 89% to 73%. The methane conversion decreased to 52% after the reaction temperature decreased to 800 °C and further decreased with an increase in the reaction time (from 52% to 45% after 50 h). When the reaction temperature decreased to 750 °C, the methane conversion decreased to 28%, and decreased further to 22% in 50 h. The reaction temperature was then decreased to 700 °C, and the methane conversion decreased to 11%, and decreased further to 9% in only 5 h. It is believed that the decreases in catalytic

activity at each temperature resulted from both the sintering of Ni nanoparticles and coking on the catalyst. Clearly, the activity and stability of ALD Ni/NP-Al₂O₃ were much lower than those of the ALD Ni/γ-Al₂O₃ catalyst, indicating that porous γ-Al₂O₃ (as compared to dense alumina nanoparticles support) was a better support for the Ni catalyst in the DRM reaction. Between each cycle, the catalyst was regenerated following the same procedures mentioned above. In the second and third cycles, the methane conversion increased at the beginning of each reaction, indicating that activation was needed for the catalyst after regeneration. The catalyst showed similar results, as compared to the first cycle. The decreases in catalytic activity at each temperature resulted from the coking of the catalyst. The reasons why the catalyst was activated at the beginning of the second and third cycles will be discussed in a later section. The average size of Ni nanoparticles increased from 3 nm to ∼37 nm after three cycles of the DRM reactions (Fig. S3). As shown in the TEM image, the alumina nanoparticle supports were sintered to form a larger particle support. The dependence of catalyst coking and Ni nanoparticles sintering on the reaction temperature was also verified (Fig. S4). The sintering of Ni nanoparticles was more severe at 850 °C, as compared to 700 °C, but coking happened under both temperatures. The DTG results (Figs. S5 and S6) showed no obvious coke content on the catalyst due to the low content of coke. Carbon nanotubes were observed on the catalyst used at 850 °C (Fig. S7). The corresponding methane reforming rates of the second cycle of the DRM reaction are shown in Table 2. In each cycle, the methane reforming rate at 700 °C was about 190 $L\,h^{-1}\,g_{Ni}^{-1}$, which was lower than the result of about 700 $L\,h^{-1}\,g_{Ni}^{-1}$ reported by Gould et al. [30]. The reason for the lower catalytic activity was believed to be the sintering of Ni nanoparticles in a series of reactions at much higher temperatures, before the reaction at 700 °C. To verify this, another reaction was carried out (directly after the reduction at 700 °C without running at higher temperatures) employing ALD Ni/NP-Al₂O₃ as the catalyst at 700 °C. The result was similar to Gould's result (Fig. S8), and the methane reforming rate was also similar to Gould's result (Table 2).

Based on this series of experiments, it was clear that the ALD Ni nanoparticles were much more active than the Ni nanoparticles synthesized by the IW method. Also, the porous γ-Al₂O₃ supported ALD Ni nanoparticle catalyst showed higher activity and greater stability, as compared to the dense alumina supported ALD Ni nanoparticle catalyst. The higher activity of the porous γ-Al₂O₃ supported catalyst could have been due to a larger number of Ni-Al₂O₃ interfacial sites formed between the Ni nanoparticles deposited inside the cavities of the porous alumina support, as compared to those of the dense alumina supported catalyst. The greater stability could have been due to the porous structure of the support, which could limit the sintering of the Ni nanoparticles and, thus, inhibit coking during the reaction. Another reason for the greater stability could have been the stronger Ni-support interaction formed by depositing Ni nanoparticles on the porous support, as compared to that of the dense substrates. Similar phenomena have also been reported. Gao et al. [37] found that the Ni nanoparticles deposited inside the cavities of the Al₂O₃ nanotubes could form more Ni-Al₂O₃ interfacial sites and stronger Ni-Al₂O₃ interac-

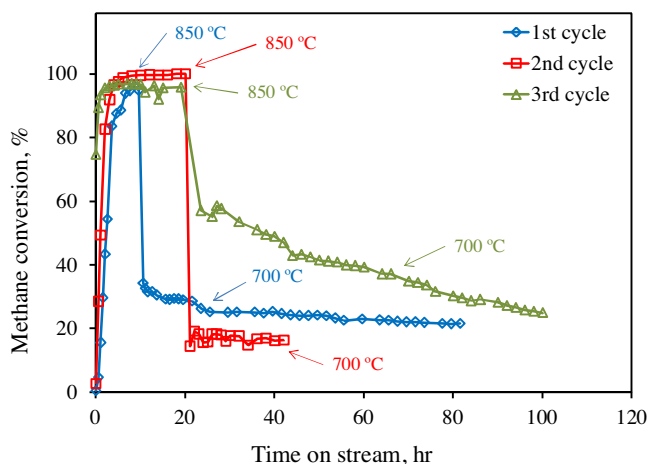**Fig. 4.** Methane conversion of dry reforming of methane catalyzed by ALD Ni/γ-Al$_2$O$_3$ at 700 °C and 850 °C.

tions, which showed higher catalytic activity and greater stability in catalyzing hydrogenation of cinnamaldehyde, as compared to that of the Ni nanoparticles deposited on the outside wall of the Al$_2$O$_3$ nanotubes by ALD. The increase in the catalytic activity of the ALD Ni/γ-Al$_2$O$_3$ catalyst at the beginning of the DRM reaction at 850 °C indicated that an activation period was needed to reduce the Ni catalyst from NiO or NiAl$_2$O$_4$ to Ni. This indicated that the catalysts can be activated at a high temperature first, and then high catalytic activity can be achieved at a lower reaction temperature (e.g., 700 °C).

The ALD Ni/γ-Al$_2$O$_3$ catalyst was first activated by running the DRM reaction at 850 °C for 10 h, and then the reaction temperature was directly decreased to 700 °C (Fig. 4). The catalyst showed activity in catalyzing the DRM reaction. In contrast, no conversion was observed for the same catalyst (after the standard reduction process) when directly employed to catalyze the DRM reaction at 700 °C. This means that the ALD Ni/γ-Al$_2$O$_3$ catalyst can be activated by the DRM reaction at 850 °C. Between each cycle, the catalyst was regenerated. In the second and third cycles, the methane conversions increased at the beginning of the reaction, which indicated that the catalyst had not been fully activated in the previous cycles of reactions. In the third cycle, the catalyst took a shorter time to recover, as compared to recovery in the second cycle. This could have been due to the fact that the catalyst was further activated in the second cycle. Compared to the results of the first batch of the catalyst (Fig. 1), the initial activity at 700 °C in the third cycle was higher, but the conversion decreased more quickly with increased reaction time. The reason for the decrease in conversion should not have been the sintering of Ni nanoparticles, since the methane conversion at 700 °C did not decrease much during the first two cycles. This decrease would have been due to the fact that the catalyst was not fully activated. These results supported our hypothesis that catalysts can be activated at a high temperature, and high catalytic activity can be achieved at a lower reaction temperature.

Chen et al. [38] previously reported that alumina supported Ni catalyst (calcined at 750 °C) showed low activity at the beginning of a DRM reaction carried out at 750 °C, but the activity increased with increased reaction time. They claimed that the increase in activity was due to the reduction of NiAl$_2$O$_4$ spinel by hydrogen produced from the DRM reaction. However, from their H$_2$-TPR results, NiAl$_2$O$_4$ spinel can hardly be reduced by hydrogen at 750 °C. Thus, the mechanism of catalyst activation should not be the reduction of NiAl$_2$O$_4$ spinel by hydrogen alone. To verify this, the ALD Ni/γ-Al$_2$O$_3$ catalyst was reduced in 20% H$_2$ and 80% Ar (with a total

flow rate of 100 sccm) at 850 °C for 10 h. It was reported that NiO could be easily reduced under these reduction conditions [13]. The reduced catalyst was applied to catalyze a DRM reaction at 700 °C; however, no conversion was observed at 700 °C. This indicated that hydrogen could not reduce/activate the catalyst at 850 °C, and the amount of reduced Ni and NiO in this catalyst was very small. Thus, the Ni content should be mainly NiAl$_2$O$_4$ spinel. The existence of NiAl$_2$O$_4$ spinel has been verified by XPS and H$_2$-TPR in a later section. However, in the DRM reaction, the methane conversion reached 90% after reaction at 850 °C for 10 h. This indicated that catalysts can be activated more easily in a mixed gas atmosphere of reaction products (e.g., H$_2$ and CO), since the DRM product at 850 °C was mainly H$_2$ and CO.

To investigate and determine the role of gases in catalyst activation, catalysts were reduced in different gases and then employed for a DRM reaction. First, one batch of a fresh catalyst was reduced in 16% H$_2$, 20% CO (H$_2$/CO ratio was similar to the gas mixture of H$_2$ and CO in the product of DRM at 850 °C) and 64% Ar (with 100 sccm of total flow rate) at 850 °C for 10 h. The catalyst was employed to catalyze the DRM reaction at 700 °C. The initial conversion was 22%, but decreased quickly to 7% in 4 h (Fig. S9). This indicated that the mixture of H$_2$ and CO was a better activator than H$_2$ alone. After 4 h of reaction at 700 °C, the reaction temperature was increased to 850 °C, and the conversion increased to 94% after about 30 h. The methane conversion at 700 °C, which was lower than that shown in the first batch (Fig. 1), kept decreasing. This could have been due to the fact that 10 h may not have been long enough for the reduction of the catalyst, or because the amounts of H$_2$ and CO introduced were not enough for the reduction process, or both. After the catalyst was regenerated, it was applied for use in the DRM reaction at 700 °C. The methane conversion was higher than that in the first cycle, indicating that the catalyst had been further activated during the first cycle of reaction at 850 °C. The fresh catalyst was also reduced in methane and the reduced catalyst showed activity in catalyzing a DRM reaction (Fig. S10). However, the methane conversion was very low (lower than 2%), indicating that the methane was also a reducing agent of the catalyst, but it was not as good as the mixture of hydrogen and carbon monoxide. It has been demonstrated that the NiAl$_2$O$_4$ spinel can be reduced by the carbon formed on the surface at a relative high temperature in a chemical-looping combustion reaction [39]. In this study, it is possible that the reduction of NiAl$_2$O$_4$ spinel in the mixed gases atmosphere of the reaction could have been partly the result of the carbon that formed on the catalyst surface from a Boudouard reaction ($2CO \rightleftharpoons CO_2 + C$) and a methane decomposition reaction ($CH_4 \rightarrow 2H_2 + C$).
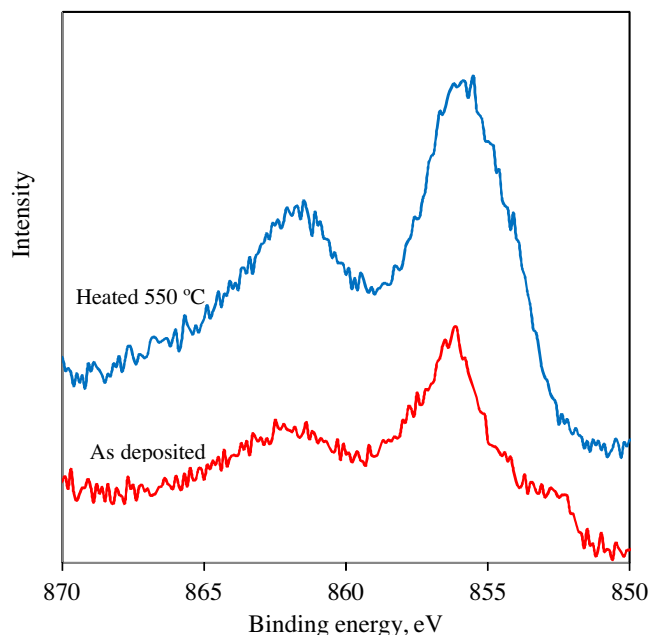
3.2. Catalysts characterization

ICP-AES results showed that the Ni loadings of ALD Ni/γ-Al$_2$O$_3$ and ALD Ni/NP-Al$_2$O$_3$ catalysts were both 0.97 wt.%. The Ni loading of the IW Ni/γ-Al$_2$O$_3$ sample was 1.15 wt.%. Fig. 5 shows the TEM image of the ALD Ni/NP-Al$_2$O$_3$ sample and the size distribution of Ni nanoparticles (inset image). The average Ni nanoparticle size was 3.6 nm, which was similar to the value reported by Gould et al. [30]. Clearly, the Ni nanoparticles were distributed uniformly on the alumina nanoparticle substrate. It is reasonable to expect that the average size of Ni nanoparticles deposited by ALD on porous γ-Al$_2$O$_3$ substrate would also be about 3.6 nm. In contrast, the size of Ni particles prepared by the IW method were normally much larger, typically by tens of nanometers [22–24].

To further verify the effect of the activation of a catalyst on DRM reaction activity, we investigated the Ni redox status of the catalyst before and after reduction. The ALD 4-Ni/γ-Al$_2$O$_3$ sample was first oxidized in air at 550 °C for 1 h, and then reduced at 850 °C in 45% H$_2$ and 55% CO (with a total flow rate of 100 sccm) for 20 h and 120 h, respectively. XPS and XRD tests were applied to these four
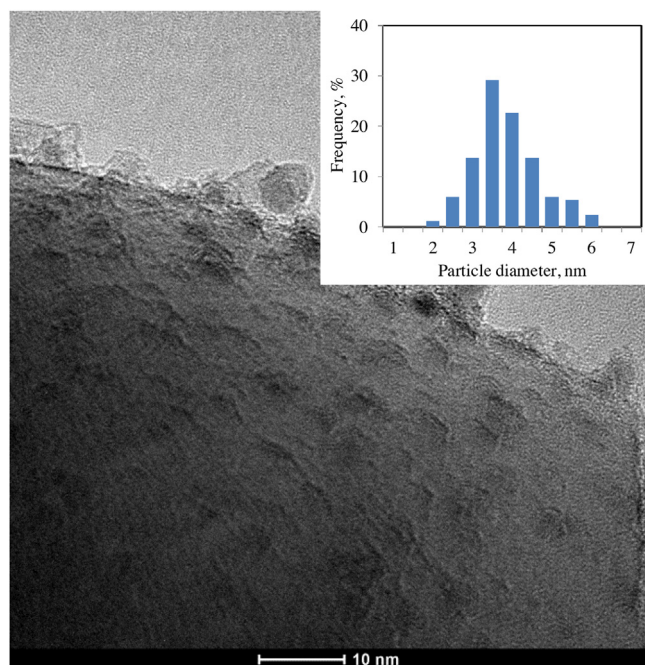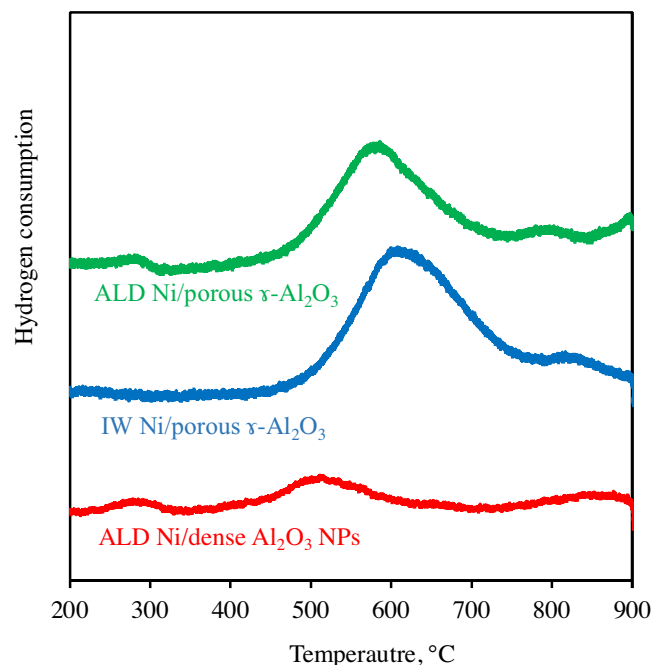
Fig. 5. TEM image of an ALD Ni/NP-Al$_2$O$_3$ catalyst. The inset image shows the size distribution of Ni nanoparticles.

Fig. 7. H$_2$-TPR results of ALD Ni/γ-Al$_2$O$_3$, IW Ni/γ-Al$_2$O$_3$, and ALD Ni/NP-Al$_2$O$_3$ catalysts.

Fig. 6. High resolution XPS spectra of nickel (2p) of the as-deposited ALD 4-Ni/γ-Al$_2$O$_3$ sample, and the sample oxidized at 550 °C for 1 h.

as-deposited, oxidized and reduced samples. Fig. 6 shows high resolution Ni (2p) XPS spectra of the ALD 4-Ni/γ-Al$_2$O$_3$ catalyst before and after being heated at 550 °C for 1 h. Metallic Ni was observed in the as-deposited ALD 4-Ni/γ-Al$_2$O$_3$ at 852.8 eV and 853.5 eV [40,41]. The NiAl$_2$O$_4$ spinel was observed at 856.2 eV [42,43], and the peak at 861.5 eV represented NiO [44]. The formation of the NiAl$_2$O$_4$ increased the interaction between Ni nanoparticles and the γ-Al$_2$O$_3$ support. The strong interaction between Ni and alumina support improved the dispersion of Ni and retarded the sintering of Ni nanoparticles [38,45]. This was the reason for the high activity and thermal stability of ALD Ni/γ-Al$_2$O$_3$. For the oxidized sample,

the metallic Ni could not be observed, while the peaks of NiO and NiAl$_2$O$_4$ became stronger. This indicated that the metallic Ni oxidized to NiO and NiAl$_2$O$_4$ during the oxidation process. Compared to the as-deposited sample, the carbon peak of the oxidized sample was weaker, indicating the removal of the residual organic component from the Ni ALD process (Fig. S11). After the oxidized sample was reduced in a mixture of H$_2$ and CO for 120 h, the Ni signal could not be detected by XPS. This was due to the fact that the Ni nanoparticles were coated by carbon formed from the Boudouard reaction. This was also verified by high resolution C (1s) XPS analysis (Fig. S11), since the carbon peak was significantly stronger after reduction. Metallic Ni could be observed by XRD in both reduced samples (Fig. S12). Based on the XPS and XRD results, it was verified that the NiAl$_2$O$_4$ spinel was formed during the ALD process and the spinel could be reduced in a mixture of CO and H$_2$ at 850 °C.

The samples were also analyzed by H$_2$-TPR. The ALD Ni/γ-Al$_2$O$_3$ and ALD Ni/NP-Al$_2$O$_3$ samples were oxidized at 550 °C for 1 h before the TPR test. As shown in Fig. 7, the H$_2$-TPR result of the ALD Ni/γ-Al$_2$O$_3$ sample analysis showed hydrogen consumption at four temperatures. The peak at 280 °C was attributed to free NiO, since the reduction temperature of a commercial NiO was reported to about 300 °C [46]. The peak at 570 °C represented the reduction of NiO that interacted with the support. Previous studies had indicated that the reduction peak of NiO that interacted with the support appeared to be within a range of 500–700 °C [47]. Generally, the reduction peak of stoichiometric NiAl$_2$O$_4$ spinel should be higher than 800 °C; therefore, a peak at 780 °C in this study could be due to the reduction of non-stoichiometric nickel aluminate [46,48]. The hydrogen consumption near 900 °C was due to reduction of the stoichiometric NiAl$_2$O$_4$ spinel, and the peak kept increasing until 900 °C. However, due to limitations of the instrument, a higher temperature H$_2$-TPR test could not be processed. Therefore, the amount of the NiAl$_2$O$_4$ could not be determined by a H$_2$-TPR test. As we know, NiO can be reduced at 700 °C, so, it was reasonable to expect that all NiO in the ALD Ni/γ-Al$_2$O$_3$ could be reduced at 700 °C. However, the catalyst that reduced at 700 °C showed no activity in catalyzing a DRM reaction at 700 °C, as we discussed earlier. Therefore, the amount of NiO in the catalyst should

have been very small and the majority of Ni in the ALD Ni/γ-Al$_2$O$_3$ catalyst should have been in the format of NiAl$_2$O$_4$. Thus, we concluded that the activation of the ALD Ni/γ-Al$_2$O$_3$ catalyst was due to the reduction of NiAl$_2$O$_4$ spinel to metallic Ni in the mixed gases atmosphere of the DRM reaction. Some NiAl$_2$O$_4$ spinel may have formed again during the regeneration process, since the NiAl$_2$O$_4$ spinel could form by calcining the catalyst at 600 °C in the presence of O$_2$ [49]. This could be the reason why the methane conversion increased at the beginnings of the second and third cycles of the DRM reactions catalyzed by ALD Ni/NP-Al$_2$O$_3$.

H$_2$-TPR tests were also employed for the IW Ni/γ-Al$_2$O$_3$ and ALD Ni/NP-Al$_2$O$_3$ samples. As shown in Fig. 7, for the ALD Ni/NP-Al$_2$O$_3$ sample, the peak at 280 °C was attributed to the reduction of free NiO. The peak for the reduction of NiO that interacted with the support at 500 °C was lower than that for the ALD Ni/γ-Al$_2$O$_3$ catalyst (570 °C). This have been due to the different morphology of the substrates. There would be more interaction between the Ni nanoparticles and the porous alumina support (concave surface), compared to the case of dense alumina particle support (convex surface). The reduction of NiAl$_2$O$_4$ spinel can be observed at 860 °C. This temperature was also lower than that of the ALD Ni/γ-Al$_2$O$_3$ catalyst, which indicated weaker interaction between Ni nanoparticles and the catalyst support. The ALD Ni/NP-Al$_2$O$_3$ catalyst showed an activity decrease during the reaction, which was due to the fact that NiO could be easily reduced to metallic Ni during the reduction process, and the Ni nanoparticles were easier to get sintered, as compared to the catalysts supported on a porous substrate.

For the IW Ni/γ-Al$_2$O$_3$ sample, no peak for free NiO was observed. This was different from what was observed for the ALD prepared catalysts. This could be due to the fact that the Ni nanoparticles synthesis methods were different. Their peaks at 600 °C and 810 °C were attributed to the reduction of NiO that interacted with the support and NiAl$_2$O$_4$ spinel, respectively. The lower reduction temperature of NiAl$_2$O$_4$ spinel indicated the weaker interaction between the Ni nanoparticles and the catalyst support as compared to the ALD Ni/γ-Al$_2$O$_3$ catalyst. The amount of the NiAl$_2$O$_4$ spinel was not much, as compared to NiO. During the catalytic reactions, it was found that the catalyst still needed a short activation period. This could have been due to the existence of NiAl$_2$O$_4$ spinel, which was not reduced during the reduction process at 700 °C, but it could have been reduced during the DRM reaction.

Ni in the format of NiAl$_2$O$_4$ is not as reactive as metallic Ni for a DRM reaction [38]. In most of the previously reported studies, the Ni/Al$_2$O$_3$ catalysts were reduced in H$_2$ at a relatively low temperature [35,36,38]. There was a high possibility that only NiO was reduced, but not the NiAl$_2$O$_4$ spinel. In the study of Gould et al. [30], the catalyst coated with five cycles of alucone MLD showed a higher steady-state methane reforming rate and better stability, as compared to the uncoated catalyst. More Ni-Al$_2$O$_3$ interfacial sites could be formed after the deposition of porous alumina films on the Ni catalyst supported on alumina nanoparticles and, thus, increased the interaction of Ni and alumina. This could be the reason why the coated catalyst prepared by Gould et al. showed higher steady-state activity. Even though it is well known that alumina is a better support for the Ni catalyst in high temperature DRM applications, due to the fact that the formation of NiAl$_2$O$_4$ could help improve the dispersion of Ni and retard the sintering of Ni nanoparticles, no report investigated the activation mechanism of the catalyst in the DRM reaction. Our study further verified that the activation/reduction of the Ni catalyst was very important for catalytic activity.

4. Conclusion

Ni nanoparticles were loaded on both dense alumina nanoparticles and porous alumina substrates. The ALD synthesized porous γ-Al$_2$O$_3$ supported Ni nanocatalyst showed both high activity and stability in the DRM reaction. The porous alumina substrate was demonstrated to be a better support for the DRM reaction, as compared to the dense alumina nanoparticles in terms of activity and stability. NiAl$_2$O$_4$ spinel was formed after Ni nanoparticles were deposited on the porous γ-Al$_2$O$_3$ by ALD. NiAl$_2$O$_4$ spinel could be reduced to metallic Ni in the DRM reaction process by CO and H$_2$ in the product of the DRM reaction, which could greatly increase catalyst activity. Methane, or the mixture of H$_2$ and CO, can reduce NiAl$_2$O$_4$ to Ni at 850 °C, but hydrogen alone cannot. This study indicates that it is feasible to deposit highly dispersed and stable Ni nanoparticles on a porous γ-Al$_2$O$_3$ support and then reduce the catalyst with a mixture of H$_2$ and CO to produce a highly stable and active catalyst for the DRM reaction.

Appendix A. Supplementary data

Supplementary data associated with this article can be found, in the online version, at http://dx.doi.org/10.1016/j.apcatb.2016.08.019.

References

[1] J. Baltrusaitis, W.L. Luyben, ACS Sustain. Chem. Eng. 3 (2015) 2100–2111.
[2] A.R.S. Darujati, W.J. Thomson, Chem. Eng. Sci. 61 (2006) 4309–4315.
[3] D.A. Wood, C. Nwaoha, B.F. Towler, J. Nat. Gas Sci. Eng. 9 (2012) 196–208.
[4] J.R. Rostrup-Nielsen, J. Sehested, J.K. Norskov, Adv. Catal. 47 (2002) 65–139.
[5] H.Y. Wang, E. Ruckenstein, Appl. Catal. A: Gen. 204 (2000) 143–152.
[6] R. Wang, H.Y. Xu, X.B. Liu, Q.J. Ge, W.Z. Li, Appl. Catal. A: Gen. 305 (2006) 204–210.
[7] A.M. O'Connor, Y. Schuurman, J.R.H. Ross, C. Mirodatos, Catal. Today 115 (2006) 191–198.
[8] S. Damyanova, B. Pawelec, K. Arishtirova, M.V.M. Huerta, J.L.G. Fierro, Appl. Catal. B: Environ. 89 (2009) 149–159.
[9] M. Wisniewski, A. Boreave, P. Gelin, Catal. Commun. 6 (2005) 596–600.
[10] P.G. Schulz, M.G. Gonzalez, C.E. Quincoces, C.E. Gigola, Ind. Eng. Chem. Res. 44 (2005) 9020–9029.
[11] C. Carrara, J. Munera, E.A. Lombardo, L.M. Cornaglia, Top. Catal. 51 (2008) 98–106.
[12] J.X. Chen, C.C. Yao, Y.Q. Zhao, P.H. Jia, Int. J. Hydrogen Energy 35 (2010) 1630–1642.
[13] M.M. Barroso-Quiroga, A.E. Castro-Luna, Int. J. Hydrogen Energy 35 (2010) 6052–6056.
[14] S. Therdthianwong, A. Therdthianwong, C. Siangchin, S. Yongprapat, Int. J. Hydrogen Energy 33 (2008) 991–999.
[15] J.R. Rostrupnielsen, J.H.B. Hansen, J. Catal. 144 (1993) 38–49.
[16] Z.Y. Hou, P. Chen, H.L. Fang, X.M. Zheng, T. Yashima, Int. J. Hydrogen Energy 31 (2006) 555–561.
[17] F. Pompeo, N.N. Nichio, M.G. González, M. Montes, Catal. Today 107–108 (2005) 856–862.
[18] H.S. Bengaard, J.K. Norskov, J. Sehested, B.S. Clausen, L.P. Nielsen, A.M. Molenbroek, J.R. Rostrup-Nielsen, J. Catal. 209 (2002) 365–384.
[19] A. Kambolis, H. Matralis, A. Trovarelli, C. Papadopoulou, Appl. Catal. A: Gen. 377 (2010) 16–26.
[20] B.Q. Xu, J.M. Wei, H.Y. Wang, K.Q. Sun, Q.M. Zhu, Catal. Today 68 (2001) 217–225.
[21] C. Courson, E. Makaga, C. Petit, A. Kiennemann, Catal. Today 63 (2000) 427–437.
[22] T. Sekino, T. Nakajima, S. Ueda, K. Niihara, J. Am. Ceram. Soc. 80 (1997) 1139–1148.
[23] D.J. Lensveld, J.G. Mesu, A.J. van Dillen, K.P. de Jong, Microporous Mesoporous Mater. 44 (2001) 401–407.
[24] P. Azadi, R. Farnood, E. Meier, J. Phys. Chem. A 114 (2010) 3962–3968.
[25] X.H. Liang, L.B. Lyon, Y.-B. Jiang, A.W. Weimer, J. Nanopart. Res. 14 (2012), article No. 943.
[26] X.H. Liang, Y. Zhou, J.H. Li, A.W. Weimer, J. Nanopart. Res. 13 (2011) 3781–3788.

[27] T.D. Gould, A.M. Lubers, B.T. Neltner, J.V. Carrier, A.W. Weimer, J.L. Falconer, J.W. Medlin, J. Catal. 303 (2013) 9–15.
[28] A. Takano, T. Tagawa, S. Goto, J. Chem. Eng. Jpn. 27 (1994) 727–731.
[29] F. Frusteri, G. Italiano, C. Espro, F. Arena, Catal. Today 171 (2011) 60–66.
[30] T.D. Gould, A. Izar, A.W. Weimer, J.L. Falconer, J.W. Medlin, ACS Catal. 4 (2014) 2714–2717.
[31] X.H. Liang, J.H. Li, M. Yu, C.N. McMurray, J.L. Falconer, A.W. Weimer, ACS Catal. 1 (2011) 1162–1165.
[32] X.H. Liang, L.F. Hakim, G.-D. Zhan, J.A. McCormick, S.M. George, A.W. Weimer, J.A. Spencer II, K.J. Buechler, J. Blackson, C.J. Wood, J. Am. Ceram. Soc. 90 (2007) 57–63.
[33] J.M. Wei, B.Q. Xu, J.L. Li, Z.X. Cheng, Q.M. Zhu, Appl. Catal. A: Gen. 196 (2000) L167–L172.
[34] Z.W. Li, L.Y. Mo, Y. Kathiraser, S. Kawi, ACS Catal. 4 (2014) 1526–1536.
[35] E. Baktash, P. Littlewood, R. Schomacker, A. Thomas, P.C. Stair, Appl. Catal. B: Environ. 179 (2015) 122–127.
[36] S.B. Wang, G.Q.M. Lu, Appl. Catal. B: Environ. 16 (1998) 269–277.
[37] Z. Gao, M. Dong, G.Z. Wang, P. Sheng, Z.W. Wu, H.M. Yang, B. Zhang, G.F. Wang, J.G. Wang, Y. Qin, Angew. Chem. Int. Ed. 54 (2015) 9006–9010.
[38] Y.G. Chen, J. Ren, Catal. Lett. 29 (1994) 39–48.
[39] T. Mattisson, M. Johansson, E. Jerndal, A. Lyngfelt, Can. J. Chem. Eng. 86 (2008) 756–767.
[40] G. Ertl, R. Hierl, H. Knozinger, N. Thiele, H.P. Urbach, Appl. Surf. Sci. 5 (1980) 49–64.
[41] A.B. Mandale, S. Badrinarayanan, S.K. Date, A.P.B. Sinha, J. Electron Spectrosc. Relat. Phenom. 33 (1984) 61–72.
[42] L. Salvati Jr., L.E. Makovsky, J.M. Stencel, F.R. Brown, D.M. Hercules, J. Phys. Chem. 85 (1981) 3700–3707.
[43] C.P. Li, A. Proctor, D.M. Hercules, Appl. Spectrosc. 38 (1984) 880–886.
[44] A.N. Mansour, Surf. Sci. Spectra 3 (1994) 231–238.
[45] Z.Y. Hou, O. Yokota, T. Tanaka, T. Yashima, Catal. Lett. 89 (2003) 121–127.
[46] J.M. Rynkowski, T. Paryjczak, M. Lenik, Appl. Catal. A: Gen. 126 (1995) 257–271.
[47] P. Kim, J.B. Joo, H. Kim, W. Kim, Y. Kim, I.K. Song, J. Yi, Catal. Lett. 104 (2005) 181–189.
[48] N. Ichikuni, D. Murata, S. Shimazu, T. Uematsu, Catal. Lett. 69 (2000) 33–36.
[49] G.H. Li, L.J. Hu, J.M. Hill, Appl. Catal. A: Gen. 301 (2006) 16–24.